



Contents lists available at ScienceDirect

Arabian Journal of Chemistry

journal homepage: www.ksu.edu.sa

Rapid screening and isolation of potential xanthine oxidase inhibitors in *Ganoderma lucidum*

Wanchao Hou¹, Xu Zhou¹, Siyuan Zhuang, Yuchi Zhang, Sainan Li^{*}, Chunming Liu^{**}

The College of Chemistry, Changchun Normal University, No. 677 North Chang-Ji Road, Changchun 130032, China

ARTICLE INFO

Keywords:

Ganoderma lucidum
Xanthine oxidase inhibitors
Chromatography
Molecular docking
Network pharmacology

ABSTRACT

Given the abundance and intricate nature of the chemical components found in natural food ingredients, functional food research has long grappled with two significant technical challenges: rapid and precise screening of active substances and targeted preparation. To enhance the efficiency of fungal food preparation, novel methodologies for screening and the production of xanthine oxidase inhibitors from *G. lucidum* have been developed. The xanthine oxidase inhibitors were rapidly screened using AUF-LC-MS. Molecular docking and molecular dynamics simulation were used to verify the anti-gout activity of active compounds. Subsequently, with activity screening as the guide, HSCCC and SPLC were employed to separate the active ingredients. Simultaneously, the mechanism of action of xanthine oxidase inhibitors was analyzed by enzymatic reaction kinetics. Finally, the anti-gout activity of chemical components in *G. lucidum* was verified by network pharmacology, and its mechanism of action was discussed. Four potential xanthine oxidase inhibitors, namely ganoderic acid C₂, B, A, and D₂, were screened from *G. lucidum*. Their docking binding energies with xanthine oxidase were -6.29, -6.65, -4.29, and -5.96 kcal/mol, respectively. The purity of the four triterpenoid active ingredients isolated from *G. lucidum* was more than 90%. These triterpenoid active ingredients showed a reversible inhibitory effect on xanthine oxidase. Network pharmacological studies revealed 71 common targets of active ingredients and gout, obtained by screening and intersecting the two targets, and identified the main metabolic pathways. The results indicate that *G. lucidum* extract can be employed for the prevention and treatment of gout disease. We enhance the efficiency and purity of active compounds preparation by incorporating enzyme inhibition assays and computerized virtual screening with compound chromatography. With this approach, we seamlessly incorporate fast discovery, screening, and focused preparation of active ingredients, as well as delving into the mechanisms of action of active monomers and proteases, and the molecular-level interactions between active ingredients and proteases. This study providing more opportunities to discover and develop new potential therapeutics from health food resources.

1. Introduction

Ganoderma lucidum (*G. lucidum*), a member of the Ganoderma taceae family and Ganoderma genus, is documented in the "Pharmacopoeia of the People's Republic of China" for its potential to boost vitality, promote relaxation, relieve cough, and stabilize respiration (Liu et al., 2016). Contemporary studies have identified a diverse array of active constituents within *G. lucidum*, including triterpenes (Yu et al., 2022a; Liu et al., 2023a), polysaccharides and proteins (Jin et al., 2020; Zhao

et al., 2023; Da et al., 2021; Wadood et al., 2023; Li et al., 2019). Clinically, it is commonly used in the treatment of chronic bronchitis, gout and adjuvant therapy after cancer chemotherapy. Simultaneously, research has demonstrated the potent anti-gout effects of ganoderic acid components. Recent years have witnessed ongoing and comprehensive investigations confirming the close association between XOD activation and gout pathogenesis (Gülšen et al., 2015; Liu and Zhang, 2005).

Gout arthritis manifests as a clinical syndrome stemming from disruptions in purine metabolism, leading to heightened uric acid

Abbreviations: XOD, xanthine oxidase; *G. lucidum*, *Ganoderma lucidum*; AUF-MS, affinity ultrafiltration mass spectrometry.

* Corresponding author.

** Corresponding author.

E-mail addresses: sainan_85@163.com (S. Li), anal_chem@sina.com (C. Liu).

¹ Co-first author, WanchaoHou and Xu Zhou contributed equally to the work.

<https://doi.org/10.1016/j.arabjc.2024.105925>

Received 25 February 2024; Accepted 21 July 2024

Available online 22 July 2024

1878-5352/© 2024 The Authors. Published by Elsevier B.V. on behalf of King Saud University. This is an open access article under the CC BY-NC-ND license (<http://creativecommons.org/licenses/by-nc-nd/4.0/>).

production or diminished excretion (Cui et al., 2022). Xanthine oxidase (XOD), a pivotal enzyme implicated in inducing hyperuricemia and elevating superoxide radical levels in the bloodstream (Wu et al., 2022). Literature indicates that *Ganoderma lucidum* triterpenoids exhibit promising traits in gout management, yet there remains a scarcity of reports on the efficacy of triterpenoid active constituents in *G. lucidum* against gout. Consequently, further exploration is warranted to elucidate the mechanisms underlying the efficacy of triterpenoid active ingredients in *G. lucidum* for gout treatment.

In the realm of natural enzyme inhibitor identification, a plethora of efficient and feasible strategies, along with innovative techniques, have surfaced. These encompass virtual screening, artificial intelligence-driven identification, spectral binding analysis, AUF with mass spectrometry, and high-throughput screening employing tailored optical substrates. Acknowledging that each technique has its unique application is crucial, as relying solely on one approach may pose limitations in terms of both accuracy and efficiency in the discovery of enzyme inhibitors. Such limitations may encompass challenges such as the occurrence of false positives, less precise screening outcomes, and a scarcity of pertinent data. The potential XOD in *G. lucidum* was examined using three distinct enzyme inhibition methods (Zhang et al., 2021). When combined with affinity ultrafiltration mass spectrometry (AUF-MS) screening methods, the limitations of *in vitro* approaches are overcome, and throughput for drug discovery is enhanced by isolating the complex from unbound compounds. Enzymatic reaction kinetics is a science that studies the rate of enzyme-catalyzed reactions and their influencing factors such as enzyme concentration, substrate concentration and inhibitors. Through enzymatic reaction kinetic research, the activity evaluation and inhibition kinetic analysis of the active ingredients with inhibitory effect can be carried out (Daniela et al., 2020). Secondly, molecular docking was employed to simulate the binding of monomeric active components to XOD. Subsequent to docking, potential proteins and specific compounds exhibiting targeted effects were identified based on the obtained results, elucidating the interaction between active ingredients and disease-related target proteins as well as their stable binding capacity (Chen et al., 2021; Abderahmane et al., 2022a). Molecular dynamics simulations, an essential tool in biomolecular computing, uses the principles of Newtonian mechanics to simulate particle trajectories and states in biomolecular systems (Abderahmane et al., 2022b). This provides comprehensive information on protein fluctuations, conformational changes, and complex dynamical processes occurring in biological systems, including protein folding and stability, conformational changes, and drug design (Abderahmane et al., 2021). And lastly, the shift from finding single targets to comprehensive network analysis has resulted in network pharmacology (Feng et al., 2023). In this study, the mechanism of action of triterpenoid active ingredients of gout in *G. lucidum* was studied through the signaling pathway of network pharmacology, which provided a basis for further clarifying its pharmacological activity and treatment mechanism. We combine AUF-MS, enzymatic reaction kinetics, molecular docking, and network pharmacology methods to screen and validate anti gout-active compounds from multiple perspectives. While experimental results' accuracy is enhanced, the amalgamation of experimental and computational methods lends greater specificity to the investigation of active compound actions.

Given the XOD inhibitory properties of *G. lucidum* extract, purified to validate their activities. In the separation of complex mixtures of triterpenoids, commonly employed techniques include column chromatography, SPLC, and CCC. HSCCC and SPLC are prevalent in modern separation fields due to their advantages of high automation and compound purity (Xiao-yan et al., 2023; Tian et al., 2023). High-speed countercurrent chromatography (HSCCC) is a liquid-liquid separation method exploiting the disparate distribution behaviors of solutes in two immiscible liquids to effect separation. In contrast to traditional techniques, HSCCC boasts attributes such as heightened efficiency, rapid separation, elevated recovery rates, superior performance, and cost-

effectiveness (Yu et al., 2022b; Song et al., 2017). Semi-preparative high performance liquid chromatography (SPLC) has the characteristics of simplicity, economy, rapidity, and easy scale-up. It has the advantages of easy operation, sample saving, fast and efficient, and is an important means for separating and preparing chemical components. The preparation amount of HSCCC is relatively higher than that of the SPLC, However, the separation precision of SPLC is much greater than that of HSCCC (Li et al., 2023). The triterpenoid active ingredients in *G. lucidum* have a complex structure and belong to lanolin derivatives, and the chemical properties and chromatographic peak time between the components are similar. For some complex target compounds, neither SPLC nor HSCCC can purify all active target compounds in one step. Consequently, the SPLC with HSCCC can be employed for the separation and purification of target active compounds with varying polarities, owing to their complementary and orthogonal characteristics. The development of this methodology enables the efficient extraction and isolation of active target compounds from the medicinal food *G. lucidum*.

We used the AUF assay to screen potential XOD inhibitors. Subsequently, the interaction types, key pathways and affinity of four target compounds with XOD were investigated by molecular docking and network pharmacology at the molecular level, and the results of UF experiments were verified simultaneously. The reaction rate, inhibition type and mechanism of different enzyme catalyzed reaction were further studied under the experimental investigation of enzymatic reaction. Finally, high purity and a large number of potential XOD inhibitors were obtained by targeted separation of HSCCC and SPLC. In this study, anti-gout pharmacologically active substances were screened and isolated from natural foods to provide support for further development of functional foods.

2. Materials and methods

2.1. Main materials and reagents

The medicinal materials of *G. lucidum* were purchased from Beijing Tong Ren Tang Medicinal Store and identified by Professor Chunming Liu (Changchun, China). Xanthine oxidase was supplied by Anwo Biotechnology Co., Ltd (Hangzhou, China). Uric acid, allopurinol, and xanthine were procured from aifa Biotechnology Co., Ltd (Chengdu, China), while ganoderic acid C₂, D₂, B, and A were obtained from YuanYe Biotechnology Co., Ltd (Shanghai, China). PBS buffer solution (Burke, Switzerland). All remaining solvents and chemicals utilized were of analytical grade and sourced from Tianjin Xinbote Chemical Corporation (Tianjin, China). The ultrafiltration chamber (100 kDa) employed was Microcon YM-100 (Bedford).

G. lucidum extract: 5.3 g *G. lucidum* extract was extracted from 500 g under the conditions of solid-liquid ratio of 1: 30 g/mL, extraction times of 2 times, ethanol concentration of 65 %, and extraction time of 1.0 h by ultrasonic method.

2.2. Main instruments and equipment

The following equipment was utilized in this study: a UPLC-Q-Exactive-MS, a TBE 300A high-speed countercurrent chromatograph, and a Waters 2489 semi-preparative liquid chromatography system. We also used an Evaluation 600 UV-Vis spectrophotometer (Thermo Scientific, USA), a Waters 2695 high-performance liquid chromatograph, and a Waters 2998 DAD detector. The analytical column employed was a SunFire™ C₁₈ (250 mm × 4.6 mm, I.D. 5 μm) from Waters, USA. Additionally, a constant temperature water bath from Beijing Tektronix Instrument Company and a centrifuge from Sigma Company, USA, were used.

2.3. Screening and binding ability of anti-gout active ingredients in *Ganoderma lucidum*

2.3.1. Screening of xanthine oxidase inhibitors by AUF-MS

The potential anti-gout active ingredients in *G. lucidum* were screened using AUF-MS, and the affinity ultrafiltration results were analyzed by calculating the binding intensity (Chen et al., 2018; Han et al., 2016). 90 μ L of XOD (0.2, 0.5, 1.0 U/mL), 30 μ L of *G. lucidum* (130 mg/mL) sample solution, and 100 μ L of 0.01 M PBS buffer were added to the incubation tube, and the mixture was incubated in a 37 °C water bath for 30 min after shaking. 220 μ L of the mixture was pipetted into an ultrafiltration tube, which was then centrifuged at 12,000 rpm for 10 min for the first time, and filtered. The ultrafiltration tube was then washed three times with PBS buffer solution, centrifuged again under the same conditions as above, and the unbound small molecule ligands and bound complexes were separated through a 100 KD filter membrane. After that, 100 μ L of 50 % methanol in water was added, the enzyme-bound triterpenoids were dissociated, centrifuged at 12,000 rpm for 10 min, and the experiment was repeated three times to obtain the active ligands. The blank test group replaced XOD with the same volume of PBS buffer, and other conditions were the same as in the experimental group, and finally the sample solution was entered into the detection system for analysis (Li et al., 2022). The binding strength (%) of the sample to XOD is calculated as follows:

$$\text{Bondstrength}(\%) = (A_y - A_k) / A_k \times 100\%$$

In the formula, A_k was the initial peak area of the compound in the original extract, A_y was the peak area of the complex bound to XOD, and the binding intensity reflects the binding ability of triterpenoids to XOD (Coşkun et al., 2022).

The UF were under vacuum, and the released ligands were analyzed by LC-MS, with the average of three parallel measurements.

2.3.2. Molecular docking and molecular dynamics simulation verification of active compounds

First, we conducted molecular docking simulations utilizing Autodock Vina 1.2.0 software to predict the XOD-binding sites of the four specified compounds and their potential post-binding conformations. We employed Autodock software for ligand processing, followed by protein hydrogenation to compute the Gasteiger charge. Subsequently, the Lamarckian genetic algorithm was applied for docking analysis of the purified compounds within Autodock Vina. The binding energy of all receptor-ligand conformations was determined, with the conformation exhibiting the lowest binding energy being designated. The docking results of the active compounds and target protein were analyzed using Python 3.4. Subsequently, the protein structures were processed using Discovery Studio 2019, and the results were visualized and analyzed to generate mock-ups (Cui et al., 2022).

Coordinates of maps = (86.515, 89.565, 137.129).

Molecular dynamics simulation was performed using Gromacs 5.1.1. The ligands were preprocessing with AmberTools22 to introduce the GAFF force field, while Gaussian 16 W was used to hydrogenate the ligands and calculate the RESP potential. The potential data is included in the topology file of the molecular dynamics system. The simulations were carried out at a constant temperature of 300 K and atmospheric pressure (1.0 Bar). Amber99sb-ildn field was employed, with water molecules (Tip3p water model) serving as the solvent. The overall charge of the simulation system was neutralized by adding an appropriate number of Na^+ ions. The free molecular dynamics simulation was performed, consisting of 5000 000 steps, each with a 2.0 fs step size, totaling a duration of 100 ns. Following the simulation, the trajectory was analyzed using software tools. The root mean square variance (RMSD), root mean square fluctuation (RMSF), and protein rotation radius of each amino acid trajectory were calculated. Moreover, MM/PBSA was calculated and a free energy morphology was plotted.

2.4. Xanthine oxidase inhibitors were separated by HSCCC coupled with SPLC

2.4.1. Distribution coefficient study

The active constituents in *G. lucidum* underwent screening and isolation using eleven solvent systems. Initial experiments were performed on each solvent system to optimize K -values for the target compounds. Once equilibrium was achieved for each solvent system, 1.0 mL of both the upper and lower phases was combined with 1.0 mg of *G. lucidum* extract in a tube and shaken until fully dissolved. The resulting two phases were filtered through a 0.45 μ m filter membrane and dissolved in 1.0 mL of methanol for subsequent analysis via HPLC (Liu et al., 2023b).

The K -values is calculated as follows:

$$K = A_{\text{upper}} / A_{\text{lower}}$$

Here, the peak area of the compound in the upper phase is denoted by A_{upper} , while the peak area of the compound in the lower phase is represented by A_{lower} .

2.4.2. HSCCC separation conditions

Following our experimental findings, the solvent system composed of ethyl acetate:*n*-butanol:water (3.0:1.0:4.0, v/v/v) was employed. The flow rate was set to 1.5 mL/min, and the rotation speed was maintained at 800 r/min. The stationary phase utilized was the upper phase of the solvent system, while the lower phase served as the mobile phase. Detection was conducted at a wavelength of 257 nm, and the sample concentration was maintained at 50 mg/mL.

2.4.3. SPLC separation conditions

In SPLC, water (A) and acetonitrile (B) were employed as mobile phases utilizing gradient elution. The mobile phase gradient program was structured as follows: 0–5 min, 10–20 % B; 5–30 min, 20–50 % B; and 30–60 min, 50–80 % B. The flow rate was sustained at 4.0 mL/min, with detection performed at a wavelength of 257 nm. An injection volume of 4.5 mL was utilized, and the crude extract of *G. lucidum* (40 mg/mL) was dissolved in a 50 % methanol aqueous solution (Xia et al., 2023).

2.4.4. Purity analysis and identification

In this investigation, LC-MS was employed to identify xanthine oxidase inhibitors in *G. lucidum*, while their purity was assessed via HPLC. Compounds within *G. lucidum* extracts were analyzed using a Waters 2695 extend C_{18} column (250 \times 4.6 mm, 5.0 μ m). The mobile phases consisted of acetonitrile (A) and water (C), employing a gradient program as follows: 0–5 min, 2 % A; 5–22 min, 2–22 % A; 22–24 min, 22 % A; 24–60 min, 22–40 % A. The flow rate was set at 0.2 mL/min, with an injection volume of 8.0 μ L. Detection was performed at a wavelength of 257 nm, and the column temperature was maintained at 30 °C.

UPLC-Q-Exactive-MS (Thermo Scientific) analysis was performed utilizing an analytical C_{18} column (100 \times 2.1 mm ID). With acetonitrile (A) and water (C), following the gradient program: 0–5 min, 2 % A; 5–20 min, 2–40 % A; 20–60 min, 40–80 % A. The flow rate was set at 0.3 mL/min, with a sample injection volume of 10 μ L. Detection was conducted at a wavelength of 257 nm, and the column temperature was maintained at 20 °C. For ionization, an electrospray ion source (ESI) was utilized in negative ion mode. The scanning range for m/z was set from 100 to 1000. Ion trap conditions included a spray voltage of 4.5 kV, nitrogen as the sheath gas auxiliary with a flow rate of 20 L/min, an ion trap pressure of 3.1×10^7 Pa, a metal capillary temperature of 350 °C, and a metal capillary voltage of 3.5 V.

2.5. Study on enzymatic reaction kinetics of xanthine oxidase inhibitors

2.5.1. Plot uric acid standard curve

The uric acid solution was injected in volumes of 2.0, 4.0, 6.0, 8.0,

10.0, 12.0, 14.0, and 16.0 μL , respectively. Subsequently, the injection volume (x) and the corresponding area (y) were employed to establish the standard curve for obtaining the regression equation.

2.5.2. Study on the inhibitory types of xanthine oxidase from active ingredients

In a 200 μL reaction system, aliquots of *G. lucidum* sample solution at concentrations of 10, 25, 50, 100, and 200 $\mu\text{mol/L}$, respectively, were dispensed at 50 μL each. Subsequently, 50 μL of XOD solution was added, and the mixture was thoroughly homogenized before being incubated in a 37 $^{\circ}\text{C}$ water bath for 10 min. Following the initial incubation, 100 μL of 0.4 mmol/L xanthine solution was introduced, thoroughly mixed, and the mixture was further incubated in a 37 $^{\circ}\text{C}$ water bath for 30 min. Subsequently, the mixture was subjected to a 10 min incubation in a 100 $^{\circ}\text{C}$ constant temperature water bath for inactivation (Zhao et al., 2021). The absorbance at a wavelength of 257 nm was measured thrice using HPLC, and the average of the three parallel measurements was considered as the experimental data.

The inhibition rate of four xanthine oxidase inhibitors in *G. lucidum* can be calculated using the following formula:

$$\text{XODInhibitionrate(\%)} = [A - (B - C)]/A \times 100\%$$

A represents the peak area of uric acid in the blank control sample, B represents the peak area of uric acid in the sample to be tested, and C represents the peak area of uric acid in the positive control sample.

2.5.3. Study on the inhibition mechanism of monomer compounds

During the enzymatic reaction, the concentration of xanthine remained constant at 0.4 mmol/L, whereas the concentrations of XOD were varied at 0.1, 0.2, 0.5, and 0.7 U/mL. This experimental setup aimed to evaluate the influence of four inhibitors on XOD activity in *G. lucidum*. A graphical representation was generated to elucidate the correlation between enzymatic reaction velocity and XOD concentration. The formation of a linear relationship passing through the origin in the plotted data signifies reversible inhibition by the inhibitor. Conversely, the appearance of a series of parallel lines intersecting the X-axis suggests irreversible inhibition (Hou et al., 2024).

In the aforementioned reaction system, the concentration of XOD was 1.0 U/mL, while the concentration of xanthine substrate was varied at 0.05, 0.10, 0.20, 0.30, and 0.40 mmol/L, respectively. Subsequently, we investigated the impact of these diverse concentrations of monomeric samples on the catalytic activity of XOD in metabolizing the xanthine. The relationship between enzymatic reaction velocity and the concentration of substrate xanthine in the reaction system was assessed. Utilizing the L-Burk double reciprocal plotting method, we constructed a linear plot of $1/V$ against $1/[S]$ under various concentrations of inhibitors. By analyzing the intersections of the plotted lines with the axes, we determined the type of inhibitory effect exerted by monomers on XOD (Liu et al., 2024).

2.6. Network pharmacology research

2.6.1. Active ingredient and disease related target prediction

G. lucidum was searched as the keyword to identify its potential active ingredients in various databases including TCMSP, TCMID, ETCM, and chemical professional databases, supplemented by published literature. The structural files for predicting active compounds were retrieved from the PubChem database and subsequently imported into the Swiss Target Prediction database for the initial prediction of component targets. Upon integration, the protein names were standardized using the Uniprot database. Finally, Cytoscape software was employed for visual analysis (Gao et al., 2024).

The keywords "gout" were inputted into the GeneCards and DrugBank databases to gather potential disease targets associated with gout. Following integration based on Score values, the targets underwent standardization through the Uniprot database.

2.6.2. Active ingredient-Gout common target construction

To explore the correlation between *G. lucidum* and targets related to gout, both drug targets and gout-related targets were uploaded to a Venn diagram website. The resultant intersection targets were subsequently imported into Cytoscape 3.6.1 software for visualization, generating a network diagram.

2.6.3. Protein-protein interaction networks construction

The obtained results were imported into the STRING database, where the PPI network was constructed. This network was saved in CSV format, facilitating the analysis of interactions between active components and gout disease targets through integrated analysis. Subsequently, the data were imported into Cytoscape 3.6.1 software for visualization, enabling the identification of potential core target genes.

2.6.4. GO and KEGG analysis

The collected targets were imported into the Metscape database with the default filter threshold set to $P < 0.01$. Subsequently, the condensed data folder was obtained, and integrated processing was conducted. The top 10 items were selected based on P -value as the next research data. Utilizing a bioinformatics platform, GO analysis and KEGG analysis were performed, and a GO and KEGG network diagram was constructed.

3. Results and discussion

3.1. Screening and binding ability of anti-gout active ingredients in *Ganoderma lucidum*

3.1.1. Screening of xanthine oxidase inhibitors by AUF-MS

As depicted in the Fig. 1, the liquid chromatographic peak areas of compounds 1, 2, 3, and 4 in the sample group with XOD were notably higher than those in the blank control sample, indicating a close association of these four compounds with xanthine oxidation enzymes. This suggests a biological affinity between these compounds and XOD, thereby speculating their potential inhibitory effect on XOD and potential anti-gout activity.

The results showed that the triterpenoid active ingredients 1, 2, 3 and 4 in *G. lucidum* combined with xanthine oxidase had significant activity (Table 1). Four potential xanthine oxidase inhibitors (namely, ganoderic acids C₂, B, A and D₂) were screened by affinity ultrafiltration experiment, and the four triterpenoid active ingredients had good binding ability with xanthine oxidase, and their binding strengths were 60.21 %, 72.63 %, 50.82 % and 55.28 %, respectively. The order of strength and weakness of the XOD inhibition effect of each active ingredient 1, 2, 3 and 4: (2) ganoderic acid B > (1) ganoderic acid C₂ > (4) ganoderic acid D₂ > (3) ganoderic acid A. In order to realize the activity verification of active ingredients 1, 2, 3 and 4, and the data analysis of the inhibition of xanthine oxidase by these four components, HPLC was further used for detection and analysis. The above method

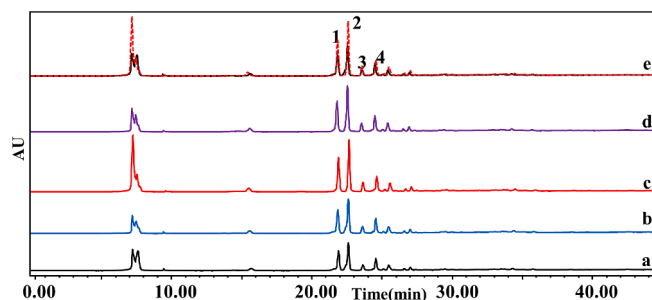


Fig. 1. High performance liquid chromatogram of *G. lucidum* combined with xanthine oxidase. a: control group, b: 0.2 U/mL, c: 0.5 U/mL, d: 1.0 U/mL, e: comparison between 0.5 U/mL XOD and control group; 1: ganoderic acid C₂, 2: ganoderic acid B, 3: ganoderic acid A, 4: ganoderic acid D₂.

Table 1
Receptor binding capacity expressed as the LC signal enhancement factor (%).^a

XOD (U/ mL)	<i>Ganoderma lucidum</i> (%) ^b			
	ganoderic acid C ₂	ganoderic acid B	ganoderic acid A	ganoderic acid D ₂
0.2	19.81	21.33	14.50	11.98
0.5	60.21	72.63	50.82	55.28
1.0	50.89	51.37	40.96	49.43

(a) Enhancement factor (%) = (compound specifically bound)/(total compound incubated) × 100 %.

(b) Extract concentration: 130 mg/mL; n = 3.

was used to detect the inhibition rate of XOD activity of triterpenoids of *G. lucidum*, and it was proved that the triterpenoids active ingredients of *G. lucidum* had inhibitory effect on XOD.

Although numerous studies have separately reported various bioactivities of ganoderic acid compounds, there have been no specific reports on the simultaneous screening of ganoderic acids C₂, B, A, and D₂ for their inhibitory effects on xanthine oxidase. Most of the literature focuses on individual ganoderic acids or employs different detection methods. Affinity ultrafiltration mass spectrometry, as an efficient screening method, provides data support for a comprehensive study of these compounds together in future research (Zhang et al., 2023).

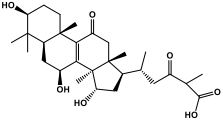
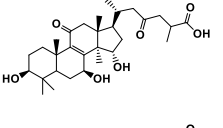
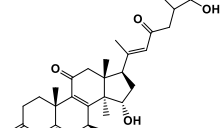
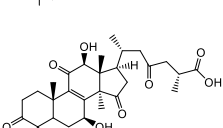
3.1.2. Simulation results of molecular docking and molecular dynamics simulation

The affinity of the four active ingredients was further validated using molecular docking techniques. The results of docking of triterpenoid active components of *G. lucidum* with XOD molecules showed that the main binding forces between the four active components and target protein were hydrogen bond or van der Waals force, accompanied by electrostatic and hydrophobic interaction. Ganoderic acid C₂ demonstrated strong interactions with PRO 132, GLN 131, and ARG 129 of XOD; ganoderic acid B exhibited significant interactions with LYS 340, VAL 313, and LYS 310; ganoderic acid A displayed notable interactions with LEU 1294, LYS 1292, THR 934, and VAL 731. Lastly, ganoderic acid D₂ showed strong interactions with ALA 1284, ALA 1281, ARG 1280, and LYS 996 of XOD amino acid residues (Fig. 2).

The docking binding energies of the triterpenoid active components ganoderic acid C₂, B, A, and D₂ were found to be −6.29, −6.65, −4.29, and −5.96 kcal/mol, respectively, for 2ckj. These docking results are consistent with the findings from ultrafiltration. Additionally, molecular docking technology confirmed their strong binding affinity with XOD (Table 2).

We calculate the RMSD for the protein, the ligand, and the protein–ligand complex RMSD by kinetic simulations (Fig. 3A1–4). For the

Table 2
Molecular docking analysis of xanthine oxidase by triterpenoid active ingredients in *G. lucidum*.

NO.	Ligand name	Ligand structure	Intermol energy (kcal/mol)	Interactions amino acid
A	ganoderic acid C ₂		−6.29	PRO132 GLN131 ARG129
B	ganoderic acid B		−6.65	LYS340 VAL313 LYS310
C	ganoderic acid A		−4.29	LEU1294 LYS1292 THR934 VAL731
D	ganoderic acid D ₂		−5.96	ALA1284 ALA1281 ARG1280 LYS996

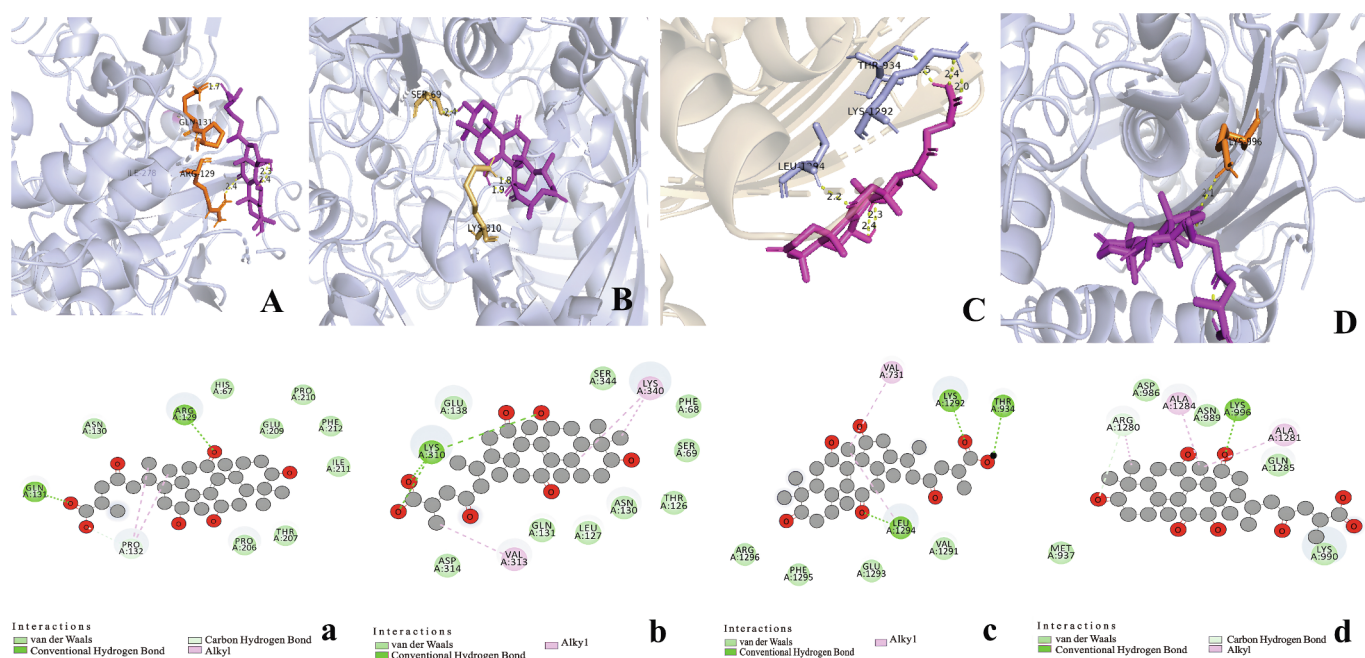


Fig. 2. Three-dimensional and two-dimensional models of four active triterpenes in *G. lucidum* by xanthine oxidase. A(a): ganoderic acid C₂; B(b): ganoderic acid B; C(c): ganoderic acid A; D(d): ganoderic acid D₂.

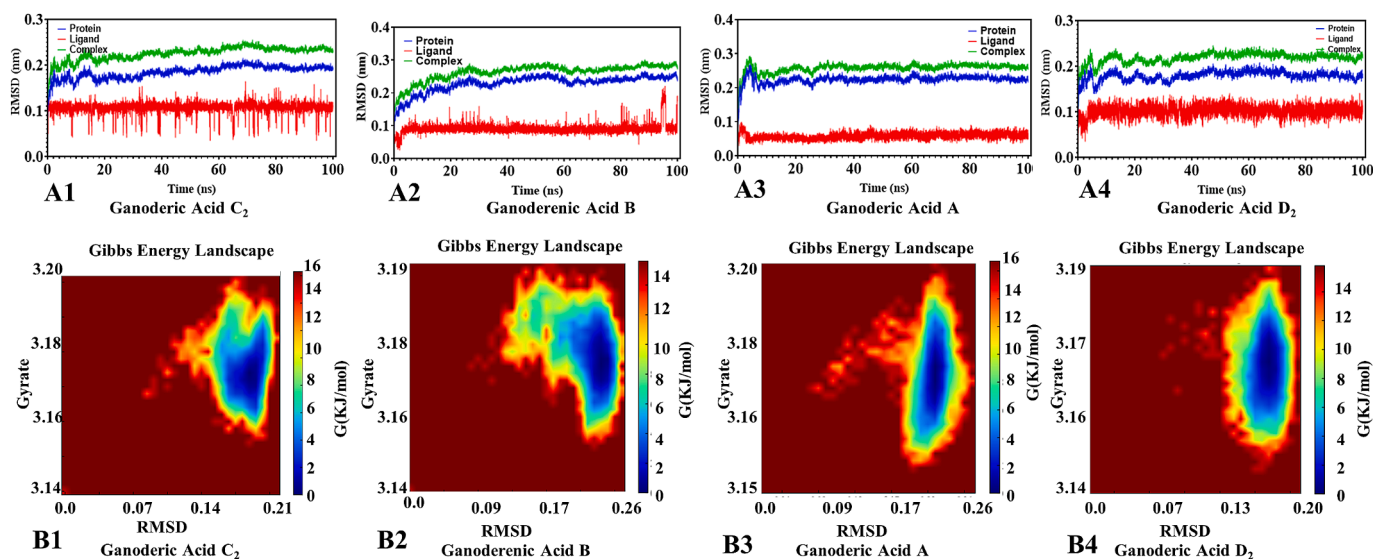


Fig. 3. RMSD and gibbs energy landscape by kinetic simulations of active compounds from *G. lucidum* were butted with xanthine oxidase. A: RMSD diagram, B: Gibbs energy landscape diagram.

initial 100 ns of the simulation, the protein–ligand RMSD values are quite high, and then gradually become steady, indicating that protein–ligand binding is stable. It can be seen that ganoderic acid D₂ has sustained small fluctuations, while the state of other small molecules RMSD is flat or remains flat after some twists and turns. On the whole, RMSD values are maintained in a small and reasonable range.

Furthermore, we analyzed Protein allostereism as shown in Fig. 3B1–4. The RMSD and cyclotron radius indicate that the protein has several lowest energy states, with blue indicating lower energy states and red signifying higher energy states. For example, if an allosteric protein has two allosteric states, it will have two lowest energy points. It is shown that during the simulation, the conjugated proteins of ganoderic acids

C₂, A, and D₂ have one allosteric state. Ganoderic acid B binds to the protein have two allosteric state allosteric state. Among these compounds, including ganoderic acid B and amino acid residues within XOD, form hydrogen bonds primarily with benzene ring hydroxyl groups. These interactions occur at key sites responsible for catalytic activity, preventing the substrate from accessing or occupying the binding site. In addition, the primary amino acid residues in ganoderic acids C₂, A, and D₂ act as proton donors in catalytic reactions and contribute to enzyme reactions through hydrogen bonding. These interactions occur relatively far from the XOD active site. Enzymes are predominantly proteins, linear macromolecules composed of peptide bonds connecting various amino acid molecules. These amino acid

Table 3
MM/GBSA computational combination free.

NO.	Ligand name	Ligand structure	Binding free energy (kcal/mol)						
			ΔE_{vdw}	ΔE_{eel}	ΔEPB	$\Delta ENPOLAR$	ΔG_{gas}	ΔG_{solv}	$\Delta TOTAL$
1	ganoderic acid C ₂		-31.56	-25.05	33.78	-4.03	-56.61	29.75	-26.86
2	ganoderic acid B		-52.64	0	35.99	-6.75	-74.98	29.24	-45.74
3	ganoderic acid A		-23.59	-23.58	33.80	-3.07	-47.17	30.73	-16.44
4	ganoderic acid D ₂		-41.43	0	38.25	-5.16	-61.11	33.09	-28.02

molecules contain functional groups such as $-NH_2$ and $-COOH$, as well as various side chains. Interactions between these amino acids involve forces such as hydrogen bonds, ionic bonds, van der Waals forces, and other attractive forces. The Table 3 provided show the energy calculations for proteins and small molecules, resulting in the total free energy of each small molecule and protein. These results can be effectively combined, with the following ranking of total free energies: ganoderic acid B (-45.74 kcal/mol) < ganoderic acid D₂ (-28.02 kcal/mol) < ganoderic acid C₂ (-26.86 kcal/mol) < ganoderic acid A (-16.44 kcal/mol). These findings indicate that monomeric components bind reversibly and non-covalently when inhibiting enzymes. Various interactions between enzymes and monomeric components induce changes in the microenvironment of enzyme secondary structures and specific amino acid residues, driven primarily by van der Waals potentials, electrostatic interactions, and hydrogen bonding.

All evidence suggests that the protein model's acceptability and good quality. These components could be the material basis for the anti-gout effect of *G. lucidum*. Molecular docking and molecular dynamics simulation techniques provides an intuitive and vivid understanding of the interaction mechanism between ligand compounds and target proteins.

3.2. Results of separation and purification

According to the experiments of XOD inhibitory results, four compounds were selected as the target compounds and then separated by HSCCC and SPLC.

3.2.1. HSCCC separation conditions

In solvent systems 1, 5, 10, and 11, the *K*-values of the target compound were notably less than 0.5, suggesting that the separation of triterpenoid components in *G. lucidum* was deemed unsuitable. It was speculated that the high polarity of the target compound might have contributed to this observation (Table 4). Therefore, *n*-butanol was incorporated into the solvent system to adjust its polarity, aiming to achieve enhanced separation efficiency for the target compound. To ensure optimal separation, a certain distance between the *K*-values of

Table 4

Partition coefficient (*K*) of the active ingredient of *G. lucidum* in different solvent systems.

NO.	Solvent system	v/v/v/v	<i>K</i> ₁	<i>K</i> ₂	<i>K</i> ₃	<i>K</i> ₄
1	<i>n</i> -hexane:ethylacetate: methanol:water	5.0:5.0:2.0:9.0	0.22	0.21	0.08	0.11
2	<i>n</i> -hexane:ethylacetate: methanol:water	5.0:5.0:3.0:7.0	Most of the compounds are in the lower layers			
3	<i>n</i> -hexane:ethylacetate: methanol:water	9.0:1.0:5.0:5.0	Most of the compounds are in the lower layers			
4	<i>n</i> -hexane:ethylacetate: methanol:water	4.0:8.0:6.0:3.0	0.03	0.10	0.35	0.45
5	<i>n</i> -hexane:ethylacetate: methanol:water	5.0:5.0:3.0:9.0	0.38	0.21	0.09	0.29
6	ethyl acetate: <i>n</i> -butanol: water	3.0:1.0:3.0	0.18	0.61	0.17	0.11
7	ethyl acetate: <i>n</i> -butanol: water	3.0:1.0:4.0	0.53	0.84	0.60	0.91
8	ethyl acetate: <i>n</i> -butanol: water	5.0:2.0:5.0	0.23	0.15	0.81	0.18
9	ethyl acetate: <i>n</i> -butanol: water	7.0:2.0:3.0	0.20	0.15	0.81	0.18
10	petroleum ether: ethylacetate:methanol: water	5.0:5.0:3.0:7.0	0.02	0.12	0.03	0.06
11	petroleum ether: ethylacetate:methanol: water	5.0:5.0:2.0:8.0	0.40	0.37	0.42	0.43
12	ethyl acetate: acetonitrile:water	5.0:2.0:5.0	0.37	0.57	0.51	0.48
13	ethyl acetate: acetonitrile:water	4.0:2.0:5.0	0.36	0.55	0.48	0.37

the target components was deemed necessary. Consequently, solvent system 7 (ethyl acetate: *n*-butanol: water, 3.0: 1.0: 4.0) was chosen for separation, with *K*-values of compounds 1, 2, 3, and 4 being determined as 0.53, 0.84, 0.60, and 0.91, respectively, falling within the appropriate range (Table 4). Ultimately, ethyl acetate: *n*-butanol: water (3.0: 1.0: 4.0, v/v/v) was deemed the optimal solvent system.

3.2.2. Separation by HSCCC

HSCCC separation was conducted for *G. lucidum* using a flow rate of 1.5 mL/min, a solvent system composed of ethyl acetate: *n*-butanol: water in a ratio of 3.0: 1.0: 4.0 (v/v/v), a rotational speed of 800 rpm, and a detection wavelength of 257 nm (Fig. 4(A)). Three compounds were isolated from a 50 mg/mL *G. lucidum* extract under single extraction conditions, identified as ganoderic acid C₂, ganoderic acid B, and ganoderic acid A, with purities of 99.10, 93.58, and 95.76 %, respectively. The stationary phase retention value was approximately 47.85 %, indicating the rapid and effective nature of HSCCC separation for *G. lucidum*.

3.2.3. Separation of active compounds by SPLC

Prior to the experiment, the experimental conditions, including the mobile phase, flow rate, and injection volume of the separation system, were optimized. Upon using water and methanol in the mobile phase, the chromatogram lacked an independent monomer peak, rendering compound separation challenging. Therefore, in this experiment, acetonitrile was selected as a substitute for methanol in the mobile phase. Subsequently, flow rates of 2.0, 4.0, 6.0, and 8.0 mL/min were compared. Eventually, a flow rate of 4.0 mL/min was chosen, the mobile phase gradient program was structured as follows: 0–5 min, 10–20 % B; 5–30 min, 20–50 % B; and 30–60 min, 50–80 % B, and the injection volume was fixed at 4.5 mL.

One triterpenoid active ingredient was isolated from *G. lucidum* by SPLC, which was ganoderic acid D₂ (purity is 90.01 %) (Fig. 4(B)).

The results demonstrated that HSCCC and SPLC, as contemporary liquid–liquid partitioning techniques, significantly improved the efficiency, purity, and selectivity of purifying active compounds from *G. lucidum*. These methods provided robust tools for effective purification, complementing the enduring value of traditional techniques in small-scale and preliminary research. The potential applications of these advanced methods in pharmaceuticals and biotechnology were substantial, particularly for extracting and purifying high-value compounds. HSCCC and SPLC, efficient separation technologies, showed excellent scalability, meeting diverse needs from laboratory to industrial production scales. Validation in small-scale experiments suggested potential for scaling up production through increased equipment capacity and optimized processes, setting a foundation for further exploration in drug development and natural product manufacturing.

3.2.4. Screening of xanthine oxidase inhibitors by AUF-MS purity analysis and identification

The triterpenoids in the *G. lucidum* extract were well separated. The four monomer compounds are ganoderic acid C₂, B, A, D₂, and the purity is 99.10, 93.58, 95.76, and 90.01 % (Fig. 4(C)).

The mass spectrometry data corresponding to the chromatographic peaks of the main compounds in the HPLC were analyzed and determined using the LC-MS method and comparison with standard products. Compound 1 exhibited a retention time of 21.49 min, with a precursor ion $[M-H]^-$ *m/z* of 517.32 in the first-order mass spectrometry. Multi-stage spectrum analysis revealed the desorption of one molecule of H₂O from the quasi-molecular ion, followed by the removal of one molecule of CO₂, generating ion fragments with *m/z* $[M-H-H_2O-CO_2]^- = 455.32$. Additionally, fragmentation information obtained through electron transfer and molecular rearrangement after ganoderic acid C₂ ionization showed peaks at *m/z* $[M-H-C_{11}H_{20}O_4]^- = 301.19$, *m/z* $[M-H-C_{12}H_{22}O_4]^- = 287.17$, and *m/z* $[M-H-C_{15}H_{20}O_3]^- = 269.18$. This fragmentation pattern aligns with reported mass

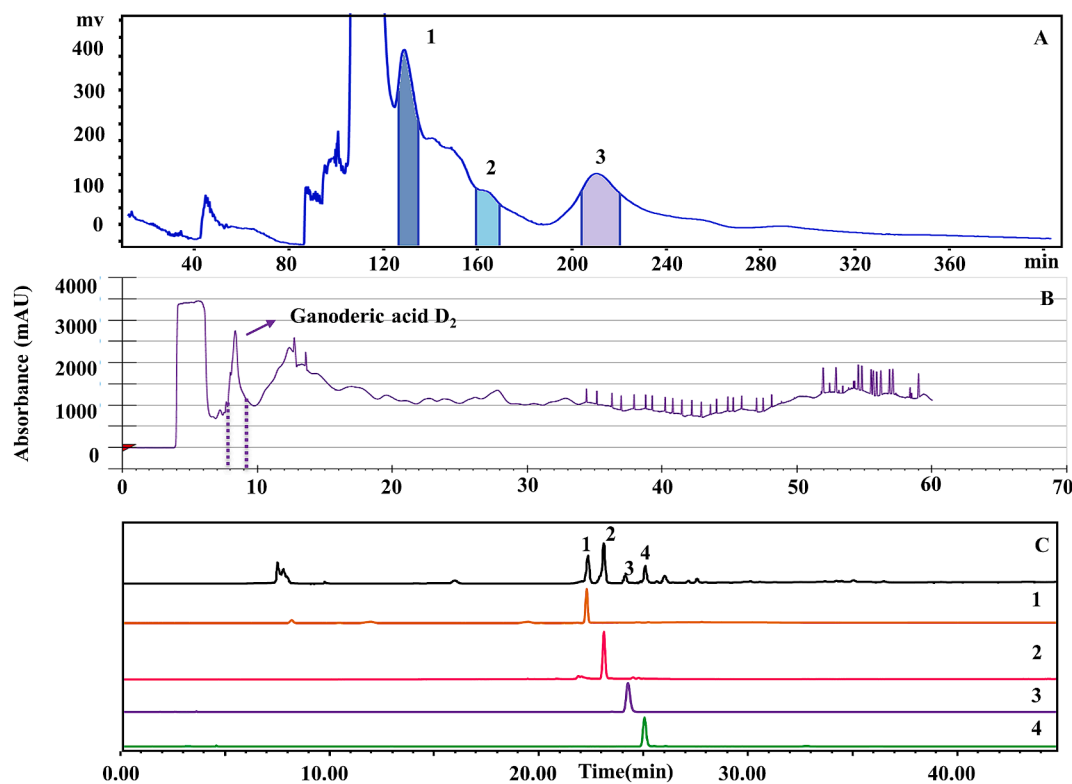


Fig. 4. HSCCC and SPLC chromatographic separation plots and separation monomer chromatographic of *G. lucidum*. A: HSCCC separation diagram, B: SPLC separation diagram, C: Liquid chromatogram of monomer composition purity; 1: ganoderic acid C₂, 2: ganoderic acid B, 3: ganoderic acid A, 4: ganoderic acid D₂.

spectrometry fragmentation information of ganoderic acid C₂ in the literature. Moreover, the retention time of compound 1 matched that of the ganoderic acid C₂ standard, indicating that this compound is likely ganoderic acid C₂ (Guo et al., 2012). Employing the same method, experimentally obtained $[M + H]^+(m/z)$ values for compounds 2 – 4 were determined to be 515, 513, and 529, respectively. Comparison of the MS data and LC retention times led to the inference that compound 2, 3, and 4 correspond to ganoderic acid B, ganoderic acid A, and ganoderic acid D₂, respectively (Zhou et al., 2013; Guo et al., 2013; Yang et al., 2007; Xu et al., 2022) (Table 5).

3.3. Enzymatic reaction analysis of active ingredients

3.3.1. Evaluation of XOD inhibitory

Taking the concentration of uric acid as the abscissa, and the peak areas of uric acid solutions of different concentrations as the ordinate, draw the standard curve of uric acid, the regression equation: $y = 672.74x - 1287.1$, $R^2 = 0.9995$, when the concentration is 2 ~ 16 $\mu\text{g/mL}$. The linearity of the standard curve was good in the range of 16 $\mu\text{g/mL}$ (method validation in the supplementary file 1).

As illustrated in the Table 6, the influence of ganoderic acid C₂, B, A, D₂, and positive controls on XOD inhibition was investigated. It can be seen from the IC₅₀ value that the four triterpenoid active ingredients in *G. lucidum* and positive controls have inhibitory effect on XOD, and

Table 5
UPLC-Q-Exactive analysis of xanthine oxidase inhibitors in *G. lucidum*.

NO.	t _R (min)	Formula	MS (m/z)	MS ² (m/z)	Compounds
1	21.49	C ₃₀ H ₄₆ O ₇	517	455,301,287,269	ganoderic acid C ₂
2	23.23	C ₃₀ H ₄₄ O ₇	515	513,451,301	ganoderic acid B
3	23.96	C ₃₀ H ₄₂ O ₇	513	453,303,285	ganoderic acid A
4	25.39	C ₃₀ H ₄₂ O ₈	529	511,467,317,301	ganoderic acid D ₂

Table 6
Inhibitory effects of monomer compounds in *G. lucidum* on XOD.

Sample	XOD Inhibition rate (%)					IC ₅₀ $\mu\text{g/mL}$
	10	25	50	100	200	
ganoderic acid C ₂	23.39	50.33	59.43	65.72	76.93	34.05
ganoderic acid B	24.03	53.11	63.91	73.61	81.27	27.94
ganoderic acid A	20.83	45.36	55.69	59.63	68.52	46.83
ganoderic acid D ₂	21.05	49.23	56.71	61.61	73.33	40.09
allopurinol	25.31	45.61	65.78	70.29	83.15	1.35

The inhibition rates were the average of the experimental results; the monomer concentrations were 10, 25, 50, 100, 200 $\mu\text{g/mL}$; the positive control drug: allopurinol (0.5, 1.0, 2.0, 5.0, 10.0 $\mu\text{g/mL}$) IC₅₀ was 1.35 $\mu\text{g/mL}$.

when the sample concentration is 10 ~ 200 $\mu\text{g/mL}$, the inhibition order of XOD by these four triterpenoids active ingredients is: ganoderic acid B (27.94 $\mu\text{g/mL}$) > ganoderic acid C₂ (34.05 $\mu\text{g/mL}$) > ganoderic acid D₂ (40.09 $\mu\text{g/mL}$) > ganoderic acid A (46.83 $\mu\text{g/mL}$).

It had been reported that plant extracts exhibiting > 50 % xanthine oxidase inhibition at 50 $\mu\text{g/mL}$ warranted further investigation (Re et al., 1999). In this study, the lowest IC₅₀ value was 46.83 $\mu\text{g/mL}$, exhibited by *G. lucidum* extract which indicating that *G. lucidum* extract could inhibit 50 % of xanthine oxidase activity at specified IC₅₀ value and showed better inhibition of xanthine oxidase activity.

3.3.2. Inhibition types and mechanisms

Identify the inhibition induced by XOD inhibitors, distinguishing between reversible and irreversible inhibition. Reversible inhibition could be categorized into C., NC., UC., and MT., (Competitive, Non-competitive, Anticompetitive, Mixed inhibition, respectively) based on the relationship among the inhibitor, substrate, and XOD. The conditions of compounds, all the plotted lines originated from the origin, with a gradual decrease as the inhibitor concentration increased, signifying a reversible inhibition (Fig. 5A1-4).

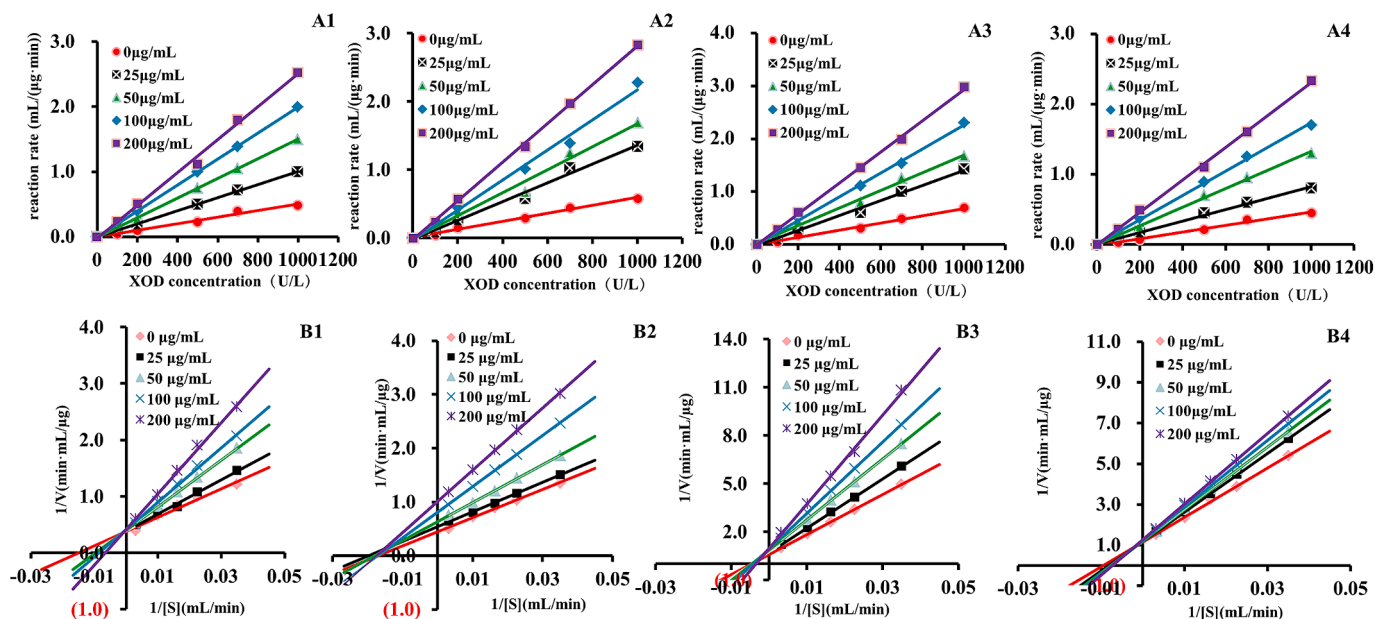


Fig. 5. Enzymatic reaction kinetics screening of active ingredients of *G. lucidum*. A: The determination curve of inhibition type that separated compounds for XOD; B: double-reciprocal plot for the determination of the inhibitory mechanism of separated compounds for XOD; 1: ganoderic acid C₂, 2: ganoderic acid B, 3: ganoderic acid A, 4: ganoderic acid D₂.

Concurrently, while maintaining a fixed of XOD at 1.0 U/mL, the xanthine was varied, and the rate of the compound was assessed at xanthine concentrations of 0.05, 0.10, 0.20, 0.30, and 0.40 mmol/L. As shown in Fig. 5B1-4, a L-Burk double reciprocal plot was constructed, with $1/V$ plotted on the vertical axis and $1/[S]$ on the horizontal axis. ganoderic acid C₂, ganoderic acid A, and ganoderic acid D₂ intersect on the Y_{axis} , this indicates that for the point corresponding to C, the intersection of the line and the Y_{axis} remains unchanged with the increase in the concentration of active ingredients, and the intercept remains nearly constant, signifying a typical competitive inhibition effect. While all straight lines of ganoderic acid B intersect on the X_{axis} , and the slope of the straight line gradually increases with the increase of active ingredients, but its intersection is always on the X_{axis} , so ganoderic acid B belongs to non-competitive inhibition. The affinity between the enzyme and the substrate could be diminished due to the competition between the compound and the substrate for the XOD catalytic site, thereby further impeding enzyme activity.

Multiple screening results consistently indicate that ganoderic acid B exhibits the strongest effect, followed by ganoderic acids C₂, D₂, and A. This efficient coupling of various screening methods provides valuable data for subsequent experiments. Ganoderic acids C₂, B, A, and D₂, as natural compounds, typically carry lower risks of adverse effects compared to synthetic drugs, making them safer options. Their inhibition of xanthine oxidase and comparison with other compounds showcase their potential in the treatment of gout. By effectively inhibiting xanthine oxidase activity, these compounds reduce the production of uric acid. This inhibitory effect helps lower uric acid levels, thereby reducing the risk of gout attacks.

3.4. Network pharmacology analysis

3.4.1. Prediction analysis of intersection target of gout and active ingredients

Based on various in vitro screening experiments, we identified four triterpenoid active components from *G. lucidum* as the material basis for disease intervention and conducted further network pharmacology studies. TCMSP, Pubchem database and Swiss Target Prediction database were used to predict the action targets of the triterpenoid active components ganoderic acid A, B, C₂ and D₂. "gout" was searched in the

GeneCards database to collect disease-related targets. As shown in Fig. 6 (A), 184 targets were obtained after deduplication by predicting compound-related targets through the database, 1780 gout disease-related targets were retrieved through the GeneCards database, and a total of 71 common targets were obtained after the analysis of the two potentially related target genes by Wayne.

3.4.2. PPI network construction and network topology analysis

Through the String platform, import the intersection gene, set the object to (Homo Sapiens), take the highest confidence level of 0.9, hide the free gene node, and obtain the protein interaction relationship. Import the results into the Cytoscape 3.9.2 software, select "Network Analyzer", and obtain the network topology parameters. Then import the downloaded TSV file into Cytoscape software to make a PPI map, and filter the top 10 core targets according to the Degree value.

After obtaining the interaction information of intersecting target proteins and removing the non-interacting targets, the network has a total of 355 edges and 39 nodes. The larger the node diameter and darker the color, the higher the node Degree value and the more target proteins interacting with it. The thicker the edges and darker the color, the stronger the interaction between the two target proteins. The Cyto NCA plug-in was used to perform topological analysis of the network, as shown in Fig. 6(B) TNF, AKT1, STAT3, EGFR, SRC, PTGS2, MMP9, MAPK3, PPARG, MAPK1, MTOR, and PPARA major targets may be closely related to gout.

G. lucidum exerted therapeutic effects in gout treatment by inhibiting TNF (tumor necrosis factor) and PTGS2 (cyclooxygenase-2), thereby reducing inflammation associated with gout. It also reduced cellular damage from oxidative stress, indirectly affecting the activity of AKT1, STAT3, and EGFR signaling pathways, contributing to alleviating symptoms and conditions of gout patients. Furthermore, it could modulate immune system function, potentially influencing the activity of SRC, MAPK (such as MAPK1, MAPK3) signaling pathways, and thereby impacting inflammation and pathological processes related to gout treatment. Additionally, it affected the activity of PPARG, MMP9, MTOR, and PPARA targets, which may have played roles in gout pathogenesis, particularly in inflammation and metabolic regulation. Its anti-inflammatory, antioxidant, and immune-modulating properties positioned it as a promising natural candidate for adjunctive treatment

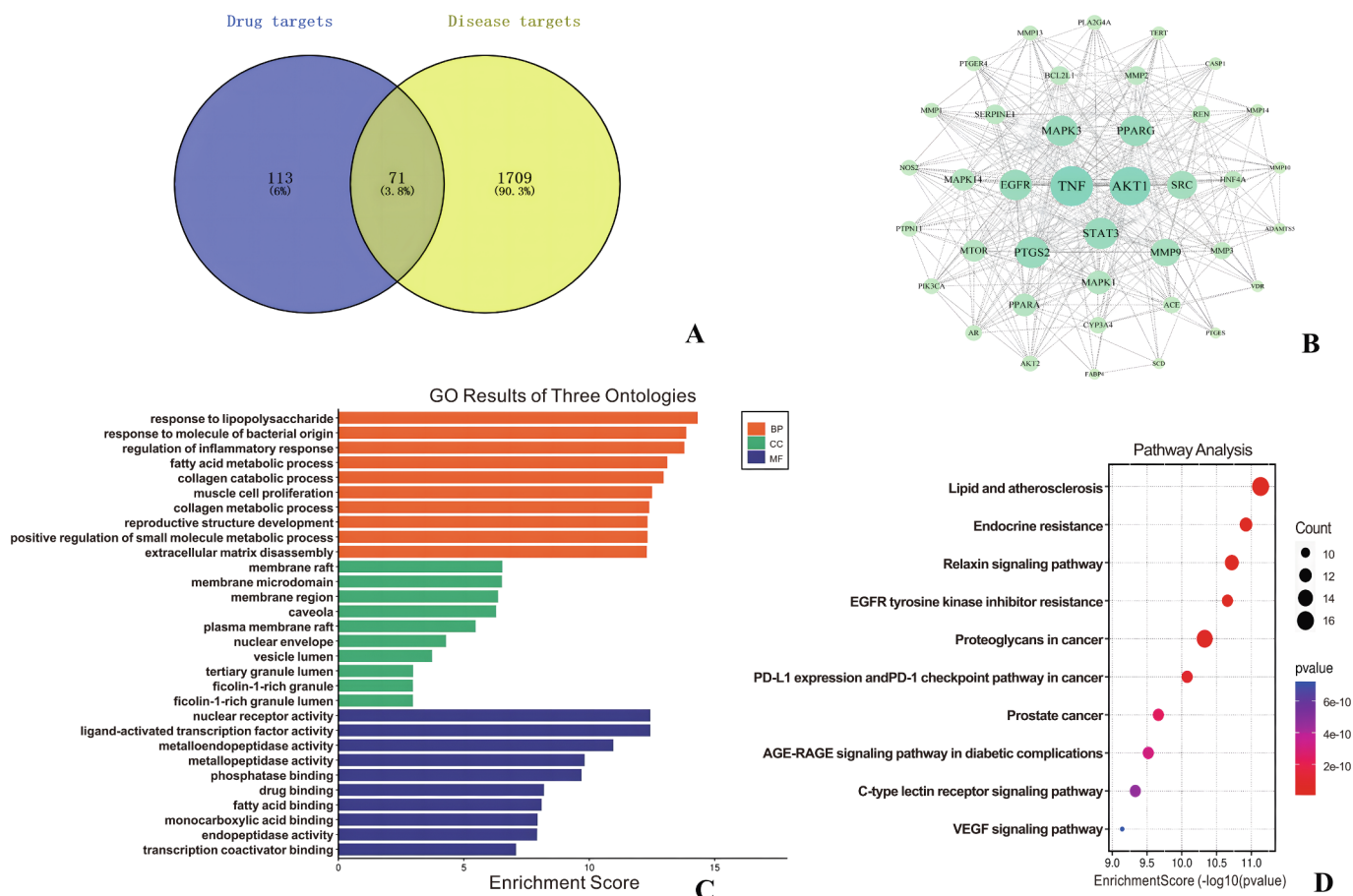


Fig. 6. Network pharmacological analysis pathway mechanism map. A: Venn diagram of Gout-target, B: PPI interaction network diagram, C: GO enrichment analysis diagram and D: KEGG action pathway analysis diagram.

in the comprehensive management of gout.

3.4.3. GO and KEGG analysis

Based on the parameters Min overlap = 3, P -value cutoff = 0.01 and Min Enrichment = 1.5 set by the metacore database, GO enrichment analysis was performed for the intersection of triterpenoid active ingredients and gout targets in *G. lucidum*.

The 71 common targets were enriched by Go enrichment to obtain Biological Process (BP), Cellular Component (CC), and Molecular Function (MF) parts. Among them, there are 995 biological process entries (response to lipopolysaccharide, response to molecule of bacterial origin, etc.), 200 cell component entries (membrane raft, membrane microdomain, etc.), and 356 molecular function items (nuclear receptor activity, etc.) (Fig. 6(C)).

There were 227 KEGG biological pathways mainly enriched by triterpenoids potential active ingredients in the treatment of gout, and the top 10 pathways were sorted by P value to obtain a bubble map of KEGG pathway analysis (Fig. 6(D)). It can be seen that target cells are mainly enriched to Lipid and atherosclerosis, Endocrine resistance, Relaxin signaling pathway, Prostate cancer and other key pathways.

These findings underscored the multifaceted pharmacological potential of *G. lucidum*'s active ingredients in addressing gout, implicating broad impacts on biological processes, cellular components, and molecular functions, as well as involvement in key pathways relevant to disease pathogenesis and treatment. Meanwhile, among the four potential active ingredients screened by network pharmacology, all of them were the four active ingredients screened by AUF-MS. And the four active components have higher degree values than other active ingredients and have more related targets, indicating that *G. lucidum* is

used in the treatment of gout. These four active components play an important role in the process of the disease. The network pharmacology results further verified the accuracy of the experiment and made the whole experimental design more complete.

4. Conclusion

In this study, AUF-MS was employed to investigate the inhibitory effects of *G. lucidum* crude extract on xanthine oxidase activity. The findings confirmed that the four primary target compounds from *G. lucidum* showed significant biological affinity towards XOD, with their inhibitory capacity displaying a positive correlation with XOD concentration. Their structures were elucidated through ESI-MSⁿ analysis. Moreover, the synergistic utilization of AUF-LC-MS and enzymatic reaction kinetics proved successful in mitigating false-positive outcomes. Through this experimental approach, the activity and content of all four target components were validated from various angles.

Additionally, molecular docking, molecular dynamics simulation, and network pharmacology analyses revealed that these four components formed hydrogen bonds or van der Waals forces, coupled with electrostatic and hydrophobic interactions with XOD amino acid residues. Seventy-one disease intersection targets of active ingredients were identified, predominantly clustered in Lipid and atherosclerosis, Endocrine resistance, and Relaxin signaling pathway, among other pivotal pathways. The activities observed for the compounds through these methods closely paralleled those determined by ultrafiltration-liquid chromatography, underscoring the necessity of employing a combination of molecular docking, molecular dynamics simulation, network pharmacology, and AUF-LC-MS for evaluating compound activities. This

integrated approach enhances comprehension of the mechanisms of action of traditional natural foods, thereby holding substantial significance for food development and research endeavors.

Furthermore, activity-oriented HSCCC and SPLC methodologies were established for the efficient and scaled-up production of potential XOD inhibitors. This approach not only effectively separated target components but also demonstrated high consistency and stability of separation results under different experimental conditions.

In conclusion, this study offers a certain theoretical basis for the future pharmacological mechanism research of *G. lucidum* and the resource development of anti-gout foods. This study provides new ideas for the search for natural anti-xanthine oxidase active ingredients. Furthermore, it provided data support for the need for more clinical research on the safety concerns and contraindications that may exist for Ganoderma extracts in clinical applications, evaluating their safety, long-term efficacy, and interactions with other medications.

Funding

This work was supported by the Natural Science Foundation of Jilin Province (NO.20240602028RC).

CRediT authorship contribution statement

Wanchao Hou: Conceptualization, Data curation, Formal analysis, Writing – original draft. **Xu Zhou:** Conceptualization, Data curation, Formal analysis, Software. **Siyan Zhuang:** Software. **Yuchi Zhang:** Methodology, Software, Supervision. **Sainan Li:** Funding acquisition, Project administration, Supervision, Writing – review & editing. **Chunming Liu:** Funding acquisition, Supervision, Writing – review & editing.

Declaration of competing interest

The authors declare that they have no known competing financial interests or personal relationships that could have appeared to influence the work reported in this paper.

Appendix A. Supplementary material

Supplementary data to this article can be found online at <https://doi.org/10.1016/j.arabjc.2024.105925>.

References

- Abderahmane, L., Khedidja, B., Leila, B., Mohamed, Y., 2021. Hispidin, Harmaline, and Harmine as potent inhibitors of bovine xanthine oxidase: Gout treatment, *in vitro*, ADMET prediction, and SAR studies. *Bioorg. Chem.* 112104937–104937 <https://doi.org/10.1016/j.bioorg.2021.104937>.
- Abderahmane, L., Talia, S., Khedidja, B., Leila, B., Mohamed, Y., Nabil, A.M., Ashraf, G. M., 2022a. Cupressus sempervirens L. flavonoids as potent inhibitors to xanthine oxidase: *in vitro*, molecular docking, ADMET and PASS studies. *J. Biomol. Struct. Dyn.* 41 (15), 11–14. <https://doi.org/10.1080/07391102.2022.2114943>.
- Abderahmane, L., Khedidja, B., Leila, B., Mohamed, Y., 2022b. The inhibitory kinetics of vitamins B9, C, E, and D₃ on bovine xanthine oxidase: Gout treatment. *Chem. Biol. Interact.* 359, 109922. <https://doi.org/10.1016/j.cbi.2022.109922>.
- Chen, G., Huang, B.X., Guo, M., 2018. Current advances in screening for bioactive components from medicinal plants by affinity ultrafiltration mass spectrometry. *Phytochem. Anal.* 29 (4). <https://doi.org/10.1002/pca.2769>.
- Chen, X., Wang, Y., Ma, Y., Wang, R., Zhao, D., 2021. To explore the Radix Paeoniae Rubra-Flos Carthami herb pair's potential mechanism in the treatment of ischemic stroke by network pharmacology and molecular docking technology. *Medicine* 100 (49). <https://doi.org/10.1097/md.00000000000027752>.
- Coşkun, Ö., Wiking, L., Yazdi, S.R., Corredig, M., 2022. Molecular details of the formation of soluble aggregates during ultrafiltration or microfiltration combined with diafiltration of skim milk. *Food Hydrocoll.* 124 <https://doi.org/10.1016/j.foodhyd.2021.107244>.
- Cui, F., Xi, L., Zhao, G., Wang, D., Tan, X., Li, J., Li, T., 2022. Screening of xanthine oxidase inhibitory peptides by ligand fishing and molecular docking technology. *Food Biosci.* 50, 102152 <https://doi.org/10.1016/j.fbio.2022.102152>.
- Da, H.R., Jwa, Y.C., Nooruddin, B.S., Kim, J.C., Lee, B., Muhammad, H., Taek, S.L., Hyoung, S.K., Soo, H.P., Chu, W.N., Kim, H.Y., 2021. Optimization of antioxidant, anti-diabetic, and anti-inflammatory activities and ganoderic acid content of differentially dried *Ganoderma lucidum* using response surface methodology. *Food Chem.* 335, 127645 <https://doi.org/10.1016/j.foodchem.2020.127645>.
- Daniela, D.B., Francesca, C., Eugenia, P., Alex, K., 2020. Enzymatic kinetic resolution of desmethylphosphinothricin indicates that phosphinic group is a bioisostere of carboxyl group. *Communications Chemistry* 3 (1), 1304–1309. <https://doi.org/10.1038/s42004-020-00368-z>.
- Feng, W., Duan, C., Pan, F., Yan, C., Dong, H., Wang, X., Zhang, J., 2023. Integration of metabolomics and network pharmacology to reveal the protective mechanism underlying Wogonoside on acute myocardial ischemia rats. *J. Ethnopharmacol.* 16871–116871 <https://doi.org/10.1016/j.jep.2023.116871>.
- Gao, J., Wang, N., Song, W., et al. 2024. Mechanisms underlying the synergistic effects of chuanxiong combined with Chishao on treating acute lung injury based on network pharmacology and molecular docking combined with preclinical evaluation. *Journal of Ethnopharmacology*, 2024, 325117862-. 10.1016/J.JEP.2024.117862.
- Gülşen, T.Ç., Mehmet, Ö., Mehmet, E.D., Mujeeb, U.R., Achyut, A., Aziz, T., Choudhary, M.L., 2015. Phytochemical investigation, antioxidant and anticholinesterase activities of *Ganoderma maadpersum*. *Ind. Crop. Prod.* 76 <https://doi.org/10.1016/j.indcrop.2015.07.042>.
- Guo, X.Y., Han, J., Ye, M., Ma, X.C., Shen, X., Xue, B.B., Che, Q.M., 2012. Identification of major compounds in rat bile after oral administration of total triterpenoids of *Ganoderma lucidum* by high-performance liquid chromatography with electrospray ionization tandem mass spectrometry. *J. Pharm. Biomed. Anal.* 63, 29–39. <https://doi.org/10.1016/j.jpba.2012.01.030>.
- Guo, X., Shen, X., Long, J., Han, J., Che, Q., 2013. Structural identification of the metabolites of ganoderic acid B from *Ganoderma lucidum* in rats based on liquid chromatography coupled with electrospray ionization hybrid ion trap and time-of-flight mass spectrometry. *Biomed. Chromatogr.* 27 (9) <https://doi.org/10.1002/bmc.2924>.
- Han, W., Zhang, X., Tian, X., Wu, G., 2016. Pharmaceutical applications of affinity-ultrafiltration mass spectrometry: Recent advances and future prospects. *J. Pharm. Biomed. Anal.* 131, 10, 1016/j.jpba.2016.09.021.
- Hou, W., Liu, Z., Zhang, Y., Li, S., Liu, C., 2024. In-depth analysis of the acetylcholinesterase inhibitors of *Ganoderma amboinense* based receptor-ligand affinity coupled with complex chromatography. *J. Food Compos. Anal.* 125105776-. <https://doi.org/10.1016/J.JFCA.2023.105776>.
- Jin, H., Song, C., Zhao, Z., Zhou, G., 2020. *Ganoderma Lucidum* Polysaccharide, an Extract from *Ganoderma Lucidum*, Exerts Suppressive Effect on Cervical Cancer Cell Malignancy through Mitigating Epithelial-Mesenchymal and JAK/STAT5 Signaling Pathway. *Pharmacology* 105 (7–8), 461–470. <https://doi.org/10.1159/000505461>.
- Li, Q.Z., Chang, Y.Z., He, Z.M., Chen, L., Zhou, X.W., 2019. Immunomodulatory activity of *Ganoderma lucidum* immunomodulatory protein via PI3K/Akt and MAPK signaling pathways in RAW264.7 cells. *J. Cell. Physiol.* 234 (12), 23337–23348. <https://doi.org/10.1002/jcp.28901>.
- Li, Y.T., Huang, T., Wang, J.Z., Yan, C.H., Gong, L.C., Wu, F.A., Wang, J., 2023. Efficient acquisition of high-purity cyanidin-3-O-glucoside from mulberry fruits: An integrated process of ATPS whole-cell transformation and semi-preparative HPLC purification. *Food Chem.* 404 <https://doi.org/10.1016/j.foodchem.2022.134651>.
- Li, J., Wang, Z., Fan, M., Hu, G., Guo, M., 2022. Potential Antioxidative and Anti-Hyperuricemic Components Targeting Superoxide Dismutase and Xanthine Oxidase Explored from *Polygonatum Sibiricum* Red. *Antioxidants* 11 (9), 1651. <https://doi.org/10.3390/antiox11091651>.
- Liu, Q., Zhuang, S., Li, S., et al. 2024. Rapid screening, isolation, and activity evaluation of potential xanthine oxidase inhibitors in *Polyporus umbellatus* and mechanism of action in the treatment of gout. *Phytochemical analysis*, 2024, 35(1):116-134. 10.1002/PCA.3279.
- Liu, J.Z., Wen, L.L., Tian, X.L., Fu, Y.J., Cui, Q.i., 2023b. An efficient two-step approach for the preparative separation and purification of eight polyphenols from *Hibiscus manihot* L. flower with high-speed countercurrent chromatography. *Arab. J. Chem.* 16 (6), 10.1016/J.ARABJC.2023.104791.
- Liu, G.Q., Zhang, K.C., 2005. Mechanisms of the Anticancer Action of *Ganoderma lucidum* (Leyss. ex Fr.) Karst.: A New Understanding. *Journal of Integrative Plant Biology* 47 (2). <https://doi.org/10.1111/j.1744-7909.2005.00037.x>.
- Liu, Y., Zhang, J., Tang, Q., Yang, Y., Xia, Y., Zhou, S., Wu, D., Zhang, Z., Dong, L., Cui, S. W., 2016. Rheological properties of β-d-glucan from the fruiting bodies of *Ganoderma lucidum*. *Food Hydrocoll.* 58 <https://doi.org/10.1016/j.foodhyd.2016.01.025>.
- Liu, Y., Zhang, D., Ning, Q., Wang, J., 2023a. Growth characteristics and metabolomics analysis of *Lactobacillus rhamnosus* GG in *Ganoderma lucidum* aqueous extract medium. *Food Biosci.* 53, 102486 <https://doi.org/10.1016/j.fbio.2023.102486>.
- Re, R., Pellegrini, N., Proteggente, A., Pannala, A., Yang, M., Rice-Evans, C., 1999. Antioxidant activity applying an improved ABTS radical cation decolorization assay. *Free Radic. Biol. Med.* 26, 1231–1237. [https://doi.org/10.1016/S0891-5849\(98\)00315-3](https://doi.org/10.1016/S0891-5849(98)00315-3).
- Song, K., Kyoung, J.L., Yeong, S.K., 2017. Development of an efficient fractionation method for the preparative separation of sesquiterpenoids from *Tussilago farfara* by counter-current chromatography. *J. Chromatogr. A* 1489, 107–114. <https://doi.org/10.1016/j.chroma.2017.02.005>.
- Tian, H., Xueli, C., Hairun, P., 2023. Overview of Solvent System Selection Strategies for Countercurrent Chromatography. *Sep. Purif. Rev.* 52 (4), 305–325. <https://doi.org/10.1080/15422119.2022.2096472>.
- Wadood, S.A., Nie, J., Li, Z., Li, C., Zhang, N., Rogers, K.M., Yuan, Y., 2023. A preliminary elemental and isotopic investigation to develop authentication tools for Chinese *Ganoderma lucidum*. *Food Control* 153, 109888. <https://doi.org/10.1016/j.foodcont.2023.109888>.
- Wu, H., Wang, Y., Ren, Z., Li, Y., Huang, J., Lin, Z., Zhang, B., 2022. Overnutrition-induced gout: An immune response to NLRP3 inflammasome dysregulation by XOD activity increased in quail. *Front. Immunol.* 13 <https://doi.org/10.3389/fimmu.2022.1074867>.

- Xia, B., Li, Y., Liu, Y., Sun, W., Chen, J., Li, L., Pang, J., Liu, X., Chen, S., Cheng, H., 2023. Rapid Separation of Asiatic Acid, Quercetin, and Kaempferol from Traditional Chinese Medicine *Centella asiatica* (L.) Urban Using HSCCC-Semi-Prep-HPLC and the Assessment of Their Potential as Fatty Acid Synthase Inhibitors. *International Journal of Analytical Chemistry* 2023, 7769368. <https://doi.org/10.1155/2023/7769368>.
- Xiao-yan, X., Mei-ting, J., Yu, W., 2023. Multiple heart-cutting two-dimensional liquid chromatography/charged aerosol detector assay of ginsenosides for quality evaluation of ginseng from diverse Chinese patent medicines. *J. Chromatogr. a* 1708, 464344. <https://doi.org/10.1016/J.CHROMA.2023.464344>.
- Xu, C., Wu, Q., Cao, Y., Lin, Y.C., Guo, W.L., Rao, P.F., Ni, L., 2022. Ganoderic acid A from *Ganoderma lucidum* protects against alcoholic liver injury through ameliorating the lipid metabolism and modulating the intestinal microbial composition. *Food Funct.* 13 (10), 5820–5837. <https://doi.org/10.1039/d1fo03219d>.
- Yang, M., Wang, X., Guan, S., Xia, J., Sun, J., Guo, H., Guo, D., 2007. Analysis of Triterpenoids in *Ganoderma lucidum* Using Liquid Chromatography Coupled with Electrospray Ionization Mass Spectrometry. *J. Am. Soc. Mass Spectrom.* 18 (5), 927–939. <https://doi.org/10.1016/j.jasms.2007.01.012>.
- Yu, P., Chen, Z., Liu, Y., Gu, Z., Wang, X., Zhang, Y., Ma, Y., Dong, M., Tian, Z., 2022b. Bioactivity-Guided Separation of Anti-Cholinesterase Alkaloids from *Uncaria rhynchophylla* (Miq.) Miq. Ex Havil Based on HSCCC Coupled with Molecular Docking. *Molecules* 27(6). DOI: 10.3390/molecules_27062013.
- Yu, X., Zhang, F.L., Li, J.R., Peng, P.Z., Liu, B., Zhao, L.N., 2022a. *Ganoderma lucidum* protease hydrolyzate on lipid metabolism and gut microbiota in high-fat diet fed rats. *Food Biosci.* 47, 101460 <https://doi.org/10.1016/j.fbio.2021.101460>.
- Zhang, Y., Sun, Y., Li, Y., 2023. Screening of xanthine oxidase inhibitors from *Ganoderma lucidum* by affinity ultrafiltration and high-performance liquid chromatography-mass spectrometry. *J. Nat. Prod.* 86 (3), 645–652. <https://doi.org/10.1021/acs.jnatprod.3c00365>.
- Zhang, X.Y., Wei, Z.J., Qiao, W.L., Sun, X.M., Jin, Z.L., Gong, W., Jia, B.X., 2021. Discovery of cyclooxygenase-2 inhibitors from *Kadsuracoccinea* by affinity ultrafiltration mass spectrometry and the anti-inflammatory activity. *Fitoterapia* 151, 104872. <https://doi.org/10.1016/j.fitote.2021.104872>.
- Zhao, C.P., Chen, G.Y., Wang, Y., Chen, H., Yu, J.W., Yang, F.Q., 2021. Evaluation of Enzyme Inhibitory Activity of Flavonoids by Polydopamine-Modified Hollow Fiber-Immobilized Xanthine Oxidase. *Molecules* (basel, Switzerland) 26 (13), 3931. <https://doi.org/10.3390/MOLECULES26133931>.
- Zhao, Y., Li, Q., Wang, M., Wang, Y., Piao, C., Yu, H., Li, Z., 2023. Structural characterization of polysaccharides after fermentation from *Ganoderma lucidum* and its antioxidant activity in HepG2 cells induced by H₂O₂. *Food Chemistry*:x 18, 100682. <https://doi.org/10.1016/j.fochx.2023.100682>.
- Zhou, Y., Xia, B., Qiu, M.H., Li, S.D., Xu, H.X., 2013. Fast analysis of triterpenoids in *Ganoderma lucidum* spores by ultra-performance liquid chromatography coupled with triple quadrupole mass spectrometry. *Biomed. Chromatogr.* 27 (11), 1560–1567. <https://doi.org/10.1002/bmc.2960>.